

# Preparation of ZTA ceramic by aqueous gelcasting with a low-toxic monomer DMAA

Chao Zhang<sup>\*</sup>, Jian Yang, Tai Qiu, Jian Guo

*College of Materials Science and Engineering, Nanjing University of Technology, Nanjing 210009, China*

Received 20 October 2011; received in revised form 2 December 2011; accepted 2 December 2011

Available online 9 December 2011

## Abstract

The present work reports the development of aqueous gelcasting of ZTA ceramic with a low-toxicity monomer DMAA. The rheological properties and the gelation behaviors of the slurries for gelcasting were investigated. It was proved that the time available for casting the slurry (idle time) can be controlled by the amounts of initiator. The ZTA green bodies exhibited a mechanical strength as high as 21 MPa. After sintered at 1600 °C for 2 h, the highest bending strength and fracture toughness of the sintered ZTA samples were as high as  $643.3 \pm 75$  MPa and  $6.3 \pm 0.3$  MPa m<sup>1/2</sup>, respectively. SEM photographs revealed that the green bodies and sintered part had a uniform microstructure. The volume fraction of tetragonal phase zirconia was as high as 90%. Dense ZTA green bodies and ceramic parts with complex shaped were produced through the new gelcasting system.

© 2011 Elsevier Ltd and Techna Group S.r.l. All rights reserved.

**Keywords:** C. Strength; DMAA; Rheological properties; ZTA

## 1. Introduction

Zirconia-toughened alumina (ZTA) ceramics are considered as promising structural materials since they have a higher crack resistance than alumina but lower price than zirconia. The applications of ZTA ceramics include bushings, cutting tool inserts, valve seats, wear components, etc. These ceramics components are usually manufactured by die pressing of alumina and zirconia powders, which is followed by sintering at elevated temperatures, then these ceramics are machined to get the desired shapes. However, this process was very expensive for preparation of complex-shaped products. As a new forming process, ceramic gelcasting has rapidly developed in the past decade. Fundamental research has been carried out by Young as well as Omatete et al. [1,2], showing the general feasibility of the process and its advantages. The advantages of the technique include high dimensional accuracy and complex shaping capabilities, as well as reducing the manufacturing cost. In this process, the powders are mixed in a pre-mixed monomer solution to get low viscosity suspension by ball-milling. After adding an initiator the

suspension is cast into a mold with the desired shape, then the entire system polymerizes in situ and green bodies with excellent mechanical property but only few percents of polymer can be obtained. Thus, the dried green bodies can be machined easily. However, industry has been reluctant to use the technique because the monomer acrylamide (AM) is a neurotoxin [3]. Many natural materials have been used in gelcasting systems like Na-alginate [4–6], chitosan [7], starch [8], agarose [9], etc., but the strength of green bodies seems inevitable in these systems. Therefore, developing new gel systems which have similar or superior properties to the AM systems, yet low toxicity has become an area of intense interest in the field for many years. N,N-dimethyl acrylamide (DMAA) is a water-soluble low-toxic reagent. Recently Zhang et al. [10] used DMAA as monomer in gelcasting system of SiC ceramics and the flexural strength of green bodies was as high as 13.9 MPa.

In the present work, gelcasting of ZTA powder was studied with DMAA as monomer. Concentrated ZTA slurry suitable for aqueous gelcasting was obtained, and high quality ZTA green bodies and dense ZTA ceramics were prepared by gelcasting and pressureless sintering. The rheological properties of ZTA slurries, and the factors affecting these properties were evaluated. The gelation properties of the ZTA suspensions as well as the properties of ceramics were also investigated.

<sup>\*</sup> Corresponding author.

E-mail address: [zhangchao1997@163.com](mailto:zhangchao1997@163.com) (C. Zhang).

## 2. Experimental procedure

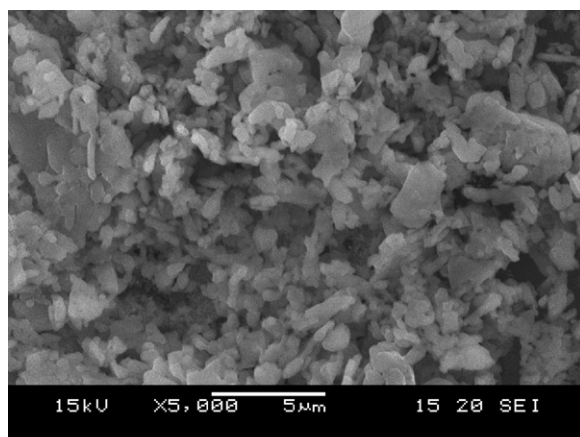
### 2.1. Raw materials

Commercially available  $\alpha$ - $\text{Al}_2\text{O}_3$  powder ( $d_{50} = 0.61 \mu\text{m}$ ) and  $\text{ZrO}_2$  powder (5.2 wt%  $\text{Y}_2\text{O}_3$ ,  $d_{50} = 0.19 \mu\text{m}$ ) were used in this investigation (Figs. 1 and 2). The polyelectrolyte SD-03 (ammonium polyacrylate, made by Nanjing University of Technology) was used as a dispersant. The analytical reagent  $\text{NH}_3 \cdot \text{H}_2\text{O}$  was used for adjusting pH value of suspensions.

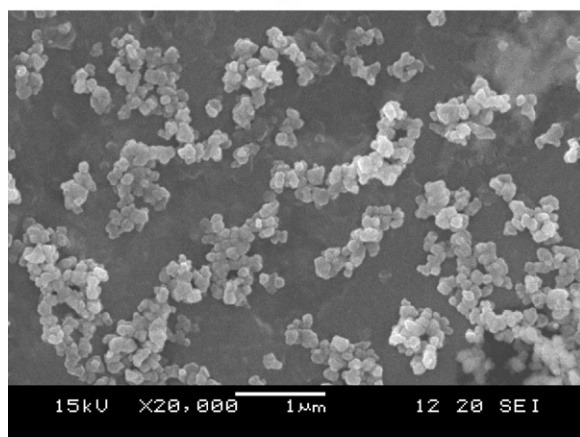
The essential components of the gelcasting process are the reactive organic monomers: mono-functional DMAA (N,N-dimethyl acrylamide, Kowa American Corporation) and difunctional MBAM (N,N'-methylenebisacrylamide). The premixed solution undergoes free-radical-initiated vinyl polymerization by an initiator  $(\text{NH}_4)_2\text{S}_2\text{O}_8$ .

### 2.2. Experimental procedure

These monomer and cross-linker were dissolved in deionized water to obtain a premixed solution ( $\text{H}_2\text{O}$ :DMAA:MBAM = 90:10:1, mass ratio). After 0.6 wt% (mass fraction of the  $\text{Al}_2\text{O}_3/\text{ZrO}_2$  powders) dispersant was added, the premixed solution was adjusted to pH 9–10 by adding  $\text{NH}_3 \cdot \text{H}_2\text{O}$ . Then the



(a)



(b)

Fig. 1. SEM photographs of  $\text{Al}_2\text{O}_3$  (a) and  $\text{ZrO}_2$  (b) powders.

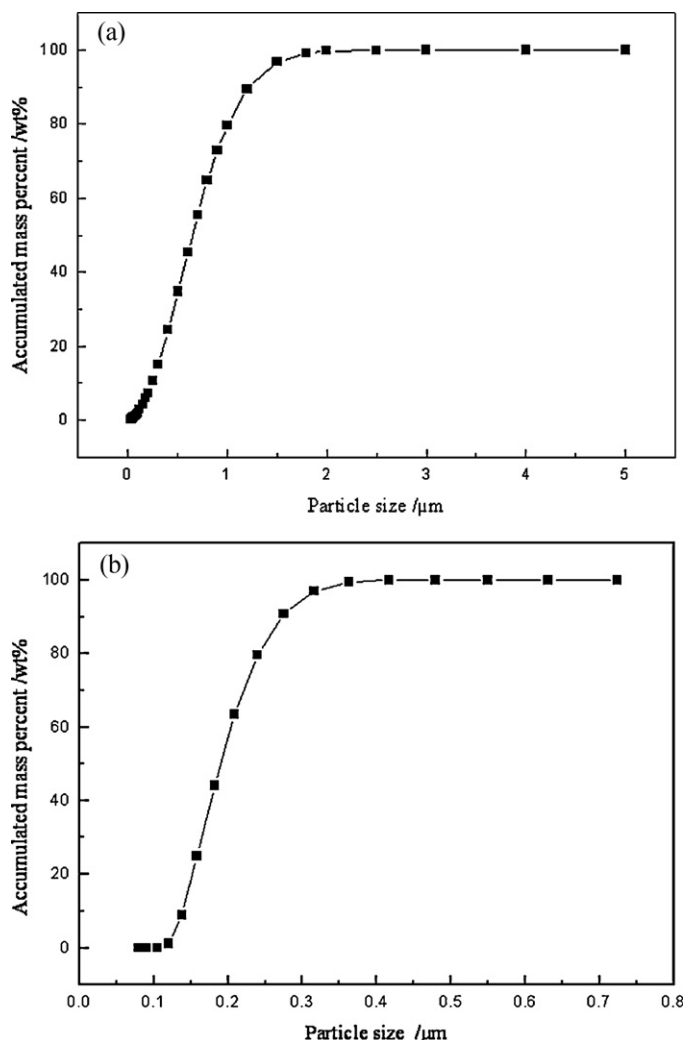


Fig. 2. Particle size distribution of  $\text{Al}_2\text{O}_3$  (a) and  $\text{ZrO}_2$  (b) powders.

solution was mixed with  $\text{Al}_2\text{O}_3$  and  $\text{ZrO}_2$  powders (mass ratio of  $\text{Al}_2\text{O}_3$  to  $\text{ZrO}_2$  is 3:1). The solid loading was 50 vol%. After mixed with zirconia ball (double mass of the  $\text{Al}_2\text{O}_3/\text{ZrO}_2$  powder), the suspensions were ball-milled for 6 h to promote dispersion, grinding and admixing process. Then 1 wt% (mass fraction of monomer) initiator (10 wt% aqueous solution) was added into the slurries which was followed by a degassing for 10 min. Finally the slurries were cast into a  $10 \text{ mm} \times 10 \text{ mm} \times 55 \text{ mm}$  stainless steel mold and kept at about  $65^\circ\text{C}$  for an hour. After the monomers polymerized, the green bodies were demolded and then dried at room temperature under controlled humidity to avoid cracking and non-uniform shrinkage. The dried green bodies were sintered at  $1600^\circ\text{C}$  for 2 h.

### 2.3. Test method

The rheological behaviors of the concentrated suspensions prepared were measured by a rotation rheometer (BROOKFIELD R/S RHEOMETER) and idle time (the time from the addition of the initiator to the commencement of polymeriza-

tion) was determined by the change of shear stress. The shear rate was  $10 \text{ s}^{-1}$  and the test temperature was  $25^\circ\text{C}$ .

Green bodies were ground into specimens of about  $3 \text{ mm} \times 4 \text{ mm} \times 40 \text{ mm}$  for the bending strength measurement using at least 5 test pieces. The pore structures and total porosity of green bodies were analyzed with the mercury intrusion method (Quantachrome company Poremaster).

The apparent porosity and relative density of sintered bodies were determined by Archimedes method. Sintered bodies were ground into specimens of about  $3 \text{ mm} \times 4 \text{ mm} \times 40 \text{ mm}$  for the bending strength measurement and specimens of about  $3 \text{ mm} \times 5 \text{ mm} \times 40 \text{ mm}$  for the toughness measurement using at least 5 test pieces, respectively. The bending strength and fracture toughness were determined by three-point bending and single edge notched beam method, respectively.

Fracture surface of green and sintered bodies were observed by scanning electron microscope (SEM, Model JSM-5900, JEO, Tokyo, Japan) to estimate the microstructure uniformity and porosity of the specimens. The phase composition of sintered body was measured by X-ray diffraction (XRD) technique on ARL X'TRA diffractometer using  $\text{Cu K}\alpha$  radiation.

### 3. Results and discussion

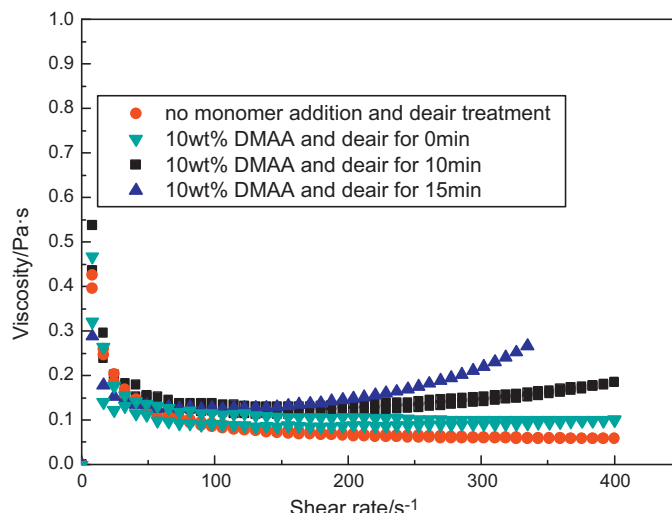
#### 3.1. Rheological properties of ZTA slurries

Fig. 3 is the rheological properties of ZTA suspensions with 10 wt% DMAA and different degassing time. From Fig. 3 we can see that, after adding 10 wt% DMAA, the viscosity of the suspension shows a little increase compared with the suspension without DMAA, and a small thixotropy occurs. The monomers may competitively adsorb on the surface of powders and influence the adsorption capacity of dispersant.

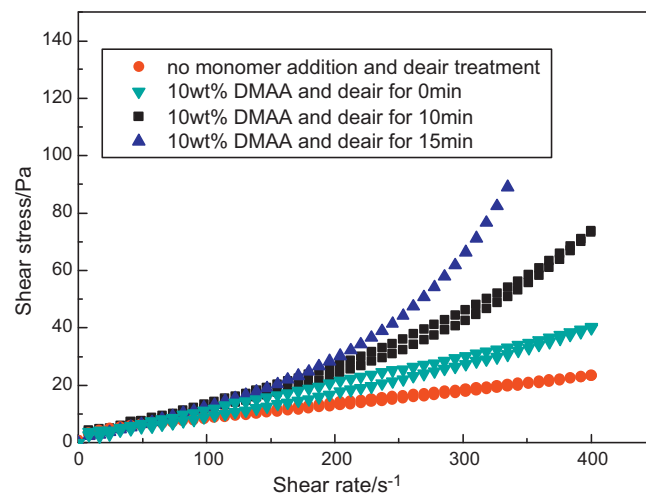
Air will be inevitably entrapped in the slurries during the preparation of slurries, which will leave pores in green bodies if it cannot be removed before casting. These pores act as flaws and jeopardize the mechanical behavior of the green and sintered bodies. In addition, the entrapped oxygen may inhibit the polymerization reaction which is also crucial to gelcasting. However, excessive deairing process will result in serious evaporation of slurries and also deteriorate the rheology properties. The optimum deairing time in this work is about 10 min, above which the rheology property of the slurries became weak with a serious shear-thick behavior which can be seen from Fig. 3.

#### 3.2. Gelation properties of the ZTA suspensions

One of the advantages of gelcasting process is a possibility to control the idle time (the time from the addition of the initiator to the commencement of polymerization). In the present study, the initiation of polymerization was determined by the changes of shear stress, the shear rate was  $10 \text{ s}^{-1}$ . This is equivalent to the time available for casting the slurry during processing. A precise determination of the idle time is very important for industrial use. Too short idle time (e.g. 10 min)



(a) Viscosity vs shear rate



(b) Shear stress vs shear rate

Fig. 3. Rheological properties of ZTA suspensions with 10 wt% DMAA and with different deairing time. (a) Viscosity vs. shear rate and (b) shear stress vs. shear rate.

can result in gelation during the mixing of initiator with the slurry and deairing process, whereas an excessively long idle time is inadvisable from economical point of view. As shown in Fig. 4, an addition of 1.5 wt% initiator, as calculated for the monomer content, resulted in a rapid gelation of the entire system. The optimum amount of initiator is about 1 wt%, which assures at least 40 min of idle time before the slurry starts to polymerize.

The effects of ZTA powders and solid loading on the idle time are shown in Fig. 5. Every suspension (also the premixed solution with on ZTA powders) was added 1.25 wt% APS (mass fraction of DMAA). From Fig. 5 we can see that gelation of the premixed solution was not observed within 1 h. On the other hand, gelation of ZTA suspensions was observed within 30 min. Moreover, the more powder contained in the slurries, the shorter idle time was observed. The catalytic effect of ceramic powder on the gelation kinetics of suspensions was

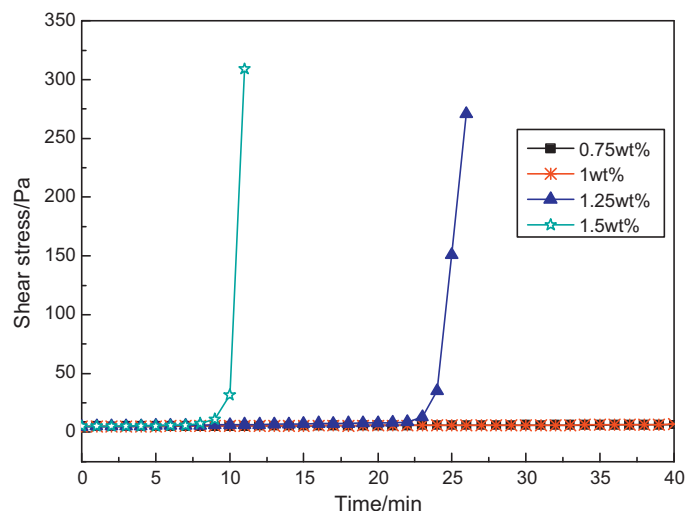


Fig. 4. Idle time as a function of initiator content.

also found by other researchers, e.g. the activation energy of free radical generation process decreases with increasing solid loading [11].

The effect of deairing process on the idle time of ZTA suspensions is shown in Fig. 6. Every suspension was added 1 wt% APS (mass fraction of DMAA). We can see that, the idle time decreased after deairing process for about 10 min. There may be two reasons for this result. First, the evaporation of slurries during deairing process leads to the increase of solid loading. Second, the inhibition function of oxygen on polymerization reaction was weak as less oxygen left in suspensions after deairing process.

### 3.3. Properties of green bodies and sintered bodies

ZTA green bodies with smooth surface and without visible defects were produced by gelcasting (Fig. 7). After drying in ovens, the flexural strength of green body can reach 21 MPa. Fig. 8 shows the corresponding structural characters of the green body. The pore structure of the green body was analyzed

with the mercury intrusion method, which can be seen from Fig. 8(a), indicates a single-peak pore distribution with a total porosity is 37.04%. A small shoulder in the range of 0.04–0.05  $\mu\text{m}$  occurred which was correspond to the volume between zircona particles which are much smaller than alumina ones, it proved that the alumina/zircona mixture was not perfect homogeneity, but, in general, the result shows a single-peak pore distribution, we could think the two particles mix homogeneously. The microstructure of the green body as observed by SEM is shown in Fig. 8(b). Particles in the green body compact closely and homogeneously. It also can be observed via SEM that particles in the green body are connected by polymer networks, which provides the green bodies with enough strength required for machining.

Table 1 shows the properties of ZTA ceramics prepared by gelcasting (solid loading is 50 vol%) and pressureless sintering. The sintering condition is 1600  $^{\circ}\text{C}$  for 2 h. Fig. 9(a) is the SEM photograph of fracture surfaces of the sintered samples which shows the dense and homogeneous microstructure. Fig. 9(b) is the corresponding back scatter electron (BSE) microphoto-

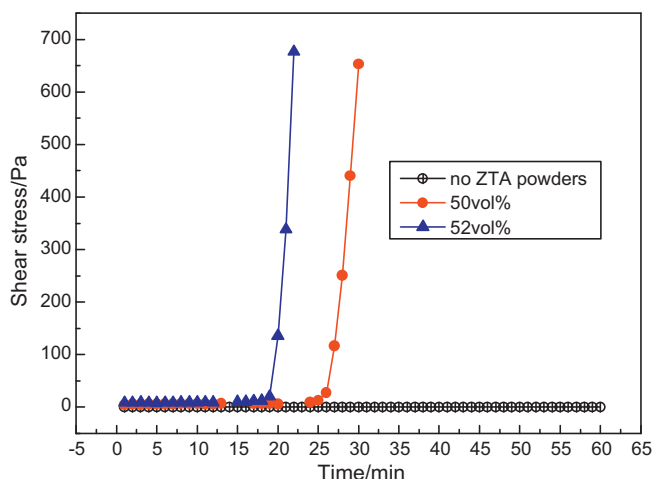


Fig. 5. Idle time as a function of solid loading.

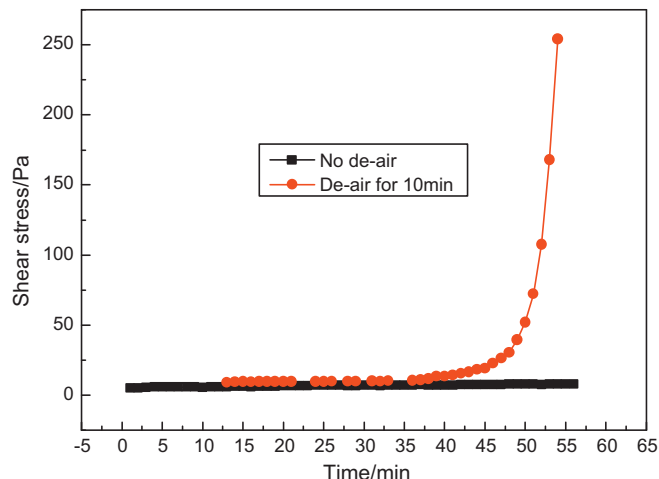


Fig. 6. The effect of deairing on the idle time of ZTA suspension.



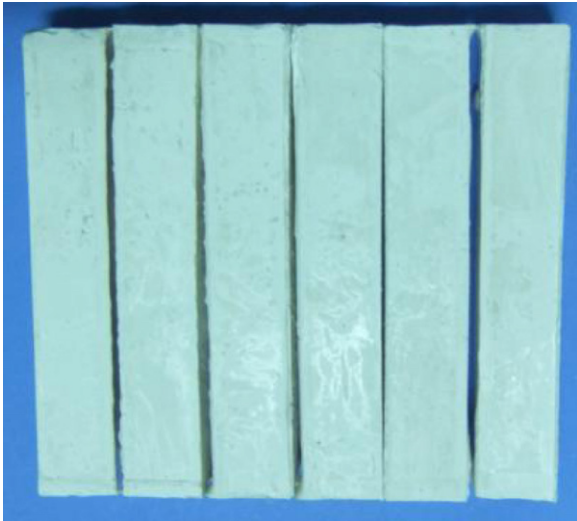


Fig. 7. Green bodies using DMAA.

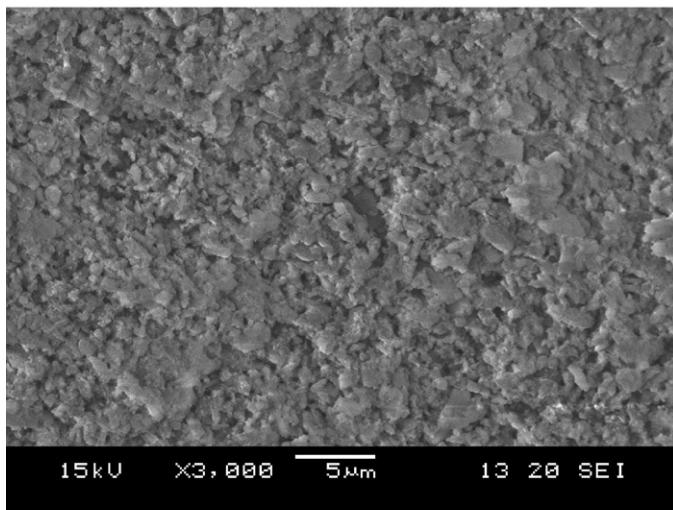
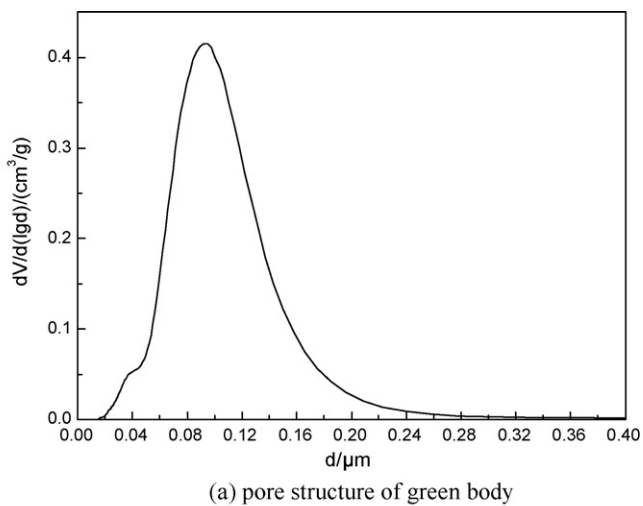


Fig. 8. Properties of green bodies by gelcasting with DMAA system. (a) Pore structure of green body and (b) SEM photograph of green body.

Table 1

The properties of ZTA ceramics.

Property	Value
Linear shrinkage/%	16.3
Apparent porosity/%	0.1
Relative density/%	98.5
Bending strength/MPa	643.3 ± 75
Fracture toughness/(MPa m <sup>1/2</sup> )	6.3 ± 0.3

graph in which the light grains are ZrO<sub>2</sub> and the black grains are Al<sub>2</sub>O<sub>3</sub>. Fig. 10 is the XRD pattern of the sintered sample, and the volume fraction of monoclinic zirconia was calculated according to the following equation [12]:

$$V_m = \frac{I_{(\bar{1}11)m} + I_{(111)m}}{I_{(\bar{1}11)m} + I_{(111)m} + I_{(111)t}}$$

where  $I$  is the integral intensity and the subscripts  $m$  and  $t$  refer to the monoclinic and tetragonal phase, respectively. According to the calculation result, the volume fraction of monoclinic zirconia is as low as 10%, which is very low in the sintered

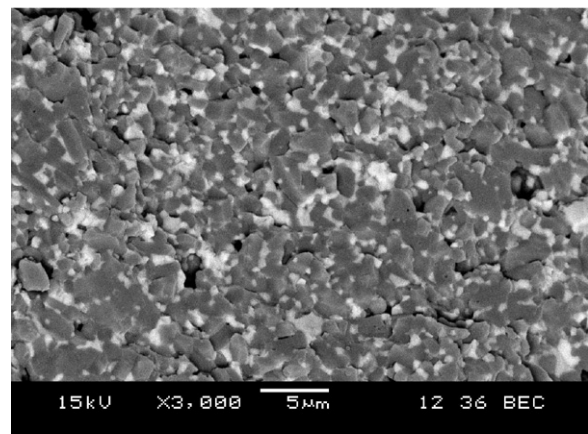
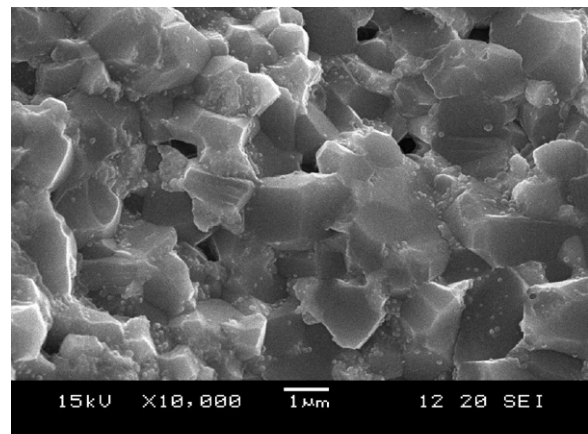


Fig. 9. SEM photographs of fracture surfaces of the sintered sample. (a) SEM photograph and (b) BSE photograph.

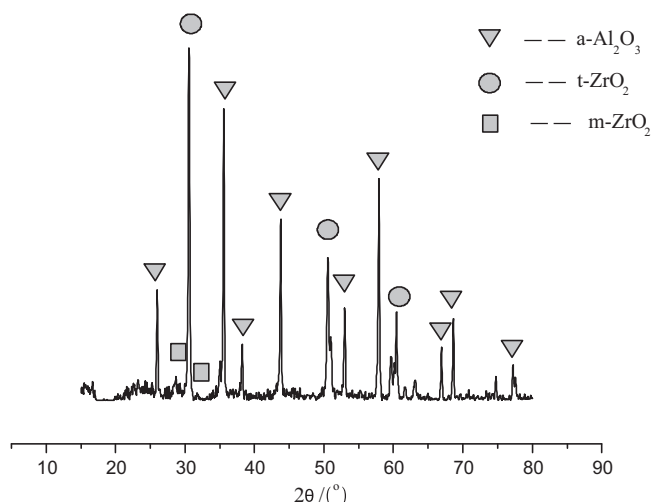


Fig. 10. XRD pattern of the sintered sample.



(a) green bodies



(b) ceramic parts

Fig. 11. Illustration of the ultimate ZTA green bodies and ceramic parts fabricated by using DMAA system. (a) Green bodies and (b) ceramic parts.

body. High tetragonal phase content and homogeneous microstructure lead to good mechanical properties. Fig. 11 is the illustration of the ultimate ZTA green bodies and ceramic parts fabricated by gelcasting using DMAA system.

#### 4. Conclusions

The present work reports the development of aqueous gelcasting of ZTA ceramic with a low-toxicity monomer DMAA. Stable and uniform ZTA slurries with 50 vol% solid content were obtained. Initiator, solid loading and deairing process all had significant effect on the idle time of the slurries. High quality green bodies with a bending strength as high as 21 MPa were prepared. SEM shows that ceramic powders in green bodies compact closely and homogeneously by the connection of polymer networks. The green body exhibited a single-peak pore size distribution as well as small pore size less than 0.3  $\mu\text{m}$ . The ZTA ceramics were also obtained by pressureless sintering at 1600  $^\circ\text{C}$  for 2 h. The linear shrinkage and relative density of ZTA sintered body are 16.3% and 98.5%, and the bending strength and toughness are  $643.3 \pm 75$  MPa and  $6.3 \pm 0.3$  MPa  $\text{m}^{1/2}$ , respectively. High tetragonal phase content and homogeneous microstructure lead to good mechanical properties.

#### Acknowledgement

This work has been supported by A Project Funded by the Priority Academic Program Development of Jiangsu Higher Education Institutions.

#### References

- [1] A.C. Young, O.O. Omatete, M.A. Janney, Gelcasting of alumina, *J. Am. Ceram. Soc.* 74 (3) (1991) 612–618.
- [2] O.O. Omatete, M.A. Janney, R.A. Strehlow, Gelcasting – a new ceramic forming process, *J. Ceram. Bull.* 70 (10) (1991) 1641–1648.
- [3] K. Cai, Y. Huang, J. Yang, Alumina gelcasting by using HEMA system, *J. Eur. Ceram. Soc.* 25 (2005) 1089–1093.
- [4] H. Akhondi, E. Taheri-Nassaj, A. Taavoni-Gilan, Gelcasting of alumina–zirconia–yttria nanocomposites with Na-alginate system, *J. Alloys Compd.* 484 (2009) 452–457.
- [5] Y. Jia, Y. Kanno, Z. Xie, Fabrication of alumina green body through gelcasting process using alginate, *J. Mater. Lett.* 57 (2003) 2530–2534.
- [6] H. Akhondi, E. Taheri-Nassaj, H. Sarpoolaky, et al., Gelcasting of alumina nanopowders based on gelation of sodium alginate, *J. Ceram. Int.* 35 (2009) 1033–1037.
- [7] M. Bengisu, E. Yilmaz, Gelcasting of alumina and zirconia using chitosan gels, *J. Ceram. Int.* 28 (2002) 431–438.
- [8] J. Chandradass, K.H. Kim, D.S. Bae, et al., Starch consolidation of alumina: fabrication and mechanical properties, *J. Eur. Ceram. Soc.* 29 (2009) 2219–2224.
- [9] I. Santacruz, M.I. Nieto, R. Moreno, Alumina bodies with near-to-theoretical density by aqueous gelcasting using concentrated agarose solutions, *J. Ceram. Int.* 31 (2005) 439–445.
- [10] T. Zhang, Z.Q. Zhang, J.X. Zhang, et al., Preparation of SiC ceramics by aqueous gelcasting and pressureless sintering, *J. Materials Science and Engineering A* 443 (2007) 257–261.
- [11] M. Potoczek, A catalytic effect of alumina grains onto polymerization rate of methacrylamide-based gelcasting system, *J. Ceram. Int.* 32 (2006) 739–744.
- [12] P. Rao, M. Iwasa, J. Wu, et al., Effect of  $\text{Al}_2\text{O}_3$  addition on  $\text{ZrO}_2$  phase composition in the  $\text{Al}_2\text{O}_3\text{--ZrO}_2$  system, *J. Ceram. Int.* 30 (2004) 923–926.